Bioinformatic Analysis of Peripheral Blood miRNA of Breast Cancer Patients in Relation With Anthracycline Cardiotoxicity

Wang Yadi
Third affiliated hospital of Jinzhou Medical University
Chen Shurui
Jinzhou Medical University
Zhang Tong
GeneScience Phamaceutical Co Ltd
Chen Suxian
Third affiliated hospital of Jinzhou Medical University
Tong Qing
Third Affiliated Hospital of Jinzhou Medical University
He Dongning (dongning129@sohu.com)
https://orcid.org/0000-0001-7127-7718

Research article

Keywords: Bioinformatics; breast cancer; cardiotoxicity; miRNA; signaling pathway.

Posted Date: October 21st, 2019

DOI: https://doi.org/10.21203/rs.2.16223/v1

Abstract

The current diagnostic methods and treatments still fail to lower the incidence of anthracycline-induced cardiotoxicity effectively. In this study, we aimed to (1) analyze the cardiotoxicity-related genes after breast cancer chemotherapy in gene expression database and (2) carry out bioinformatic analysis to identify cardiotoxicity-related abnormal expressions, the biomarkers of such abnormal expressions, and the key regulatory pathways after breast cancer chemotherapy. Cardiotoxicity-related gene expression data (GSE40447) after breast cancer chemotherapy was acquired from the GEO database. The biomarker expression data of women with chemotherapy-induced cardiotoxicity (group A), chemotherapy history but no cardiotoxicity (group B), and confirmatory diagnosis of breast cancer but normal ejection fraction before chemotherapy (group C) were analyzed to obtain the mRNA with differential expressions and predict the miRNAs regulating the differential expressions. The miRanda formula and functional enrichment analysis were used to screen abnormal miRNAs. Then, the gene ontology (GO) analysis was adapted to further screen the miRNAs related to cardiotoxicity after breast cancer chemotherapy. The data of differential analysis of biomarker expression of groups A, B, and C using the GSE40447-related gene expression profile database showed that there were 30 intersection genes. The differentially expressed mRNAs were predicted using the miRanda and TargetScan software, and a total of 2978 miRNAs were obtained by taking the intersections. Further, the GO analysis and targeted regulatory relationship between miRNA and target genes were used to establish miRNA-gene interaction network to screen and obtain 7 cardiotoxicity-related miRNAs with relatively high centrality, including hsa-miR-4638-3p, hsa-miR-5096, hsa-miR-4763-5p, hsa-miR-1273g-3p, hsa-miR6192, hsa-miR-4726-5p and hsa-miR-1273a. Among them, hsa-miR-4638-3p and hsa-miR-1273g-3p had the highest centrality. The PCR verification results were consistent with those of the chip data. There are differentially expressed miRNAs in the peripheral blood of breast cancer patients with anthracycline cardiotoxicity. Among them, hsa-miR-4638-3p and hsa-miR-1273g-3p are closely associated with the onset of anthracycline cardiotoxicity in patients with breast cancer. Mining, integrating, and validating effective information resources of biological gene chips can provide a new direction for further studies on the molecular mechanism of anthracycline cardiotoxicity.

Background

Combined treatment based on anthracyclines, such as doxorubicin, epirubicin, and pirarubicin, is usually the standard regimen for the first-line treatment of breast cancer. It has definite therapeutic effect and is indispensable. However, cardiotoxicity is the most serious side effect of anthracyclines. Both clinical research and practical observations have shown that cardiotoxicity induced by anthracyclines is often progressive and irreversible [1,2]. Cardiac injury might occur even when anthracyclines are used for the first time. Therefore, it is particularly important to actively prevent the cardiotoxicity induced by anthracyclines. Currently, the therapeutic effect on patients with anthracycline-induced cardiotoxicity is highly limited. The current diagnostic methods and treatment levels still fail to lower the incidence of anthracycline-induced cardiotoxicity effectively. This is because anthracycline-induced cardiotoxicity is a

complicated, multifactorial, and multistep biological process. The existing research achievements are not sufficient to fully reveal the mechanism of its incidence and development. It is important to identify methods for the early specific diagnosis and effective prognosis.

During recent years, the use of high-throughput methods to detect gene expression has become a common practice. Microarray chip technology can quantify tens of thousands of gene transcript information simultaneously. The gene expression omnibus (GEO) is currently the largest public high-throughput molecular abundance expression database globally. It mainly stores gene expression data. The GEO allows researchers to upload, download, save, and retrieve different types of genomic data.

In the present study, we aimed to (1) analyze the cardiotoxicity-related genes after breast cancer chemotherapy in gene expression database and (2) carry out bioinformatic analysis to identify cardiotoxicity-related abnormal expressions, the biomarkers of such abnormal expressions, and the key regulatory pathways after breast cancer chemotherapy.

Materials and Methods

Data mining and analysis

GEO database mining and chip dataset acquisition

Chip samples were screened from the GEO database (http://www.ncbi.nlm.nih.gov/geo/) of the National Center for Biotechnology Information (NCBI) (accession number: GSE40447). The chip was from the Affymetrix human genome U133A platform, containing 22,283 gene probes. The chip data was submitted by McCaffrey et al. (PMID: 23630447; 2013), and included patients with confirmatory diagnosis of breast cancer: women with anthracycline-induced cardiotoxicity, chemotherapy history but no cardiotoxicity, and normal ejection fraction before chemotherapy. According to the test results, the raw data in these chips were divided into group A (female breast cancer patients with anthracycline-induced cardiotoxicity), group B (female breast cancer patients with chemotherapy history but no cardiotoxicity), and group C (female breast cancer patients with normal ejection fraction before chemotherapy).

Data preprocessing and differential expression analysis

For each sample, the gene expression value of all the probes was reduced to a relatively absolute average gene expression value. Subsequently, we estimated the missing data and carried out quantile normalization of the data. The R-value of the differentially expressed genes was determined. To avoid false positive results caused by multiple test problems, Benjamin Hochberg method was used to correct the primary *P*-value to the false discovery rate (FDR). The FDR < 0.05 was adopted as the cut off.

GO analysis and DGE analysis

The GO analysis is used to generate a dynamic controlled vocabulary (character table) that can be applied to all studies on eukaryotic genomes. It is often used to study and analyze large-scale genome

and transcriptome data. The DEG data were divided into two groups—the up-regulated and down-regulated groups based on gene overexpression. Subsequently, the GO analysis was performed using the gene set analysis toolkit. The difference was considered statistically significant when $P < 0.05$.

Enrichment analysis

Regarding the functional annotation of DEGs, the enrichment expression of KEGG pathway has been defined by KAAS[3]. The difference was considered statistically significant when $P < 0.05$.

miRNAs expression detection by real-time quantitative PCR

Research sample: 10 tubes (3 mL/tube) of frozen blood of patients with breast cancer that was collected before and after chemotherapy respectively and stored in low-temperature refrigerators (-80°C) were randomly sampled from the First Affiliated Hospital and Third Affiliated Hospital of Jinzhou Medical University from May 2017 to August 2018.

Reagents: The miRNA-specific extraction kit (miRNeasy mini kit) was purchased from Qiagen, Germany; the miRNA reverse transcription kit was purchased from Takara (Dalian, China); the q-PCR kit was purchased from TransGen Biotech (Beijing,China); and the miRNA primers were designed and synthesized by Changchun Jing Mei Biological Engineering Co. Ltd. (Changchun, China).

Instruments: The Nanodrop 2000 ultra-micro spectrophotometer (Thermo, USA), Stepone quantitative PCR instrument (ABI, USA); and Bioptic Qsep100 automatic nucleic acid analyzer (BiOptic, Taiwan).

RT and q-PCR detection of miRNA expression: The miRNA extracted from the plasma was reverse transcribed into cDNA according to the instructions provided in the Takara reverse transcription kit. The corresponding RT primers were then added. The subsequent quantitative-polymerase chain reaction (q-PCR) was carried out using the SYBR Green PCR kit with the synthesized cDNA as the template. The reaction conditions were as follows: preheating at 95°C for 10 min, followed by heating at 95°C for 15 s and 60°C for 1 min with a total of 40 cycles. Using U6 as the reference, the Ct value, dissolution curve, and amplification curve of the samples were analyzed after the experiment.The following primer sets were used for qRT-PCR: miR4638-3P:TGGACACCGCTCAGCCGG; miR1273g-3P:ACCACTGCACTCCAGCCTGAG; U6:CTCGCTTCGGCAGCACA.

Statistical analyses

The SPSS 17.0 statistical software was used for data analysis. The measurement data with normal distribution are expressed as mean ± standard deviation ($X \pm SD$), and two-independent-sample *t* test was used for comparison between groups. The measurement data with non-normal distribution are expressed as median (interquartile range, IQR), and Wilcoxon rank sum test was used for comparison between groups. The χ^2 test was used to compare the enumeration data between the groups. The difference was statistically significant when $P < 0.05$.

Methods

Data mining and analysis

GEO database mining and chip dataset acquisition

Chip samples were screened from the GEO database (http://www.ncbi.nlm.nih.gov/geo/) of the National Center for Biotechnology Information (NCBI) (accession number: GSE40447). The chip was from the Affymetrix human genome U133A platform, containing 22,283 gene probes. The chip data was submitted by McCaffrey et al. (PMID: 23630447; 2013), and included patients with confirmatory diagnosis of breast cancer: women with anthracycline-induced cardiotoxicity, chemotherapy history but no cardiotoxicity, and normal ejection fraction before chemotherapy. According to the test results, the raw data in these chips were divided into group A (female breast cancer patients with anthracycline-induced cardiotoxicity), group B (female breast cancer patients with chemotherapy history but no cardiotoxicity), and group C (female breast cancer patients with normal ejection fraction before chemotherapy).

Data preprocessing and differential expression analysis

For each sample, the gene expression value of all the probes was reduced to a relatively absolute average gene expression value. Subsequently, we estimated the missing data and carried out quantile normalization of the data. The R-value of the differentially expressed genes was determined. To avoid false positive results caused by multiple test problems, Benjamin Hochberg method was used to correct the primary *P*-value to the false discovery rate (FDR). The FDR < 0.05 was adopted as the cut off.

GO analysis and DGE analysis

The GO analysis is used to generate a dynamic controlled vocabulary (character table) that can be applied to all studies on eukaryotic genomes. It is often used to study and analyze large-scale genome and transcriptome data. The DEG data were divided into two groups—the up-regulated and down-regulated groups based on gene overexpression. Subsequently, the GO analysis was performed using the gene set analysis toolkit. The difference was considered statistically significant when $P < 0.05$.

Enrichment analysis

Regarding the functional annotation of DEGs, the enrichment expression of KEGG pathway has been defined by KAAS[3]. The difference was considered statistically significant when $P < 0.05$.

miRNAs expression detection by real-time quantitative PCR

Research sample: 10 tubes (3 mL/tube) of frozen blood of patients with breast cancer that was collected before and after chemotherapy respectively and stored in low-temperature refrigerators (-80°C) were randomly sampled from the First Affiliated Hospital and Third Affiliated Hospital of Jinzhou Medical University from May 2017 to August 2018.

Reagents: The miRNA-specific extraction kit (miRNeasy mini kit) was purchased from Qiagen, Germany; the miRNA reverse transcription kit was purchased from Takara (Dalian, China); the q-PCR kit was purchased from TransGen Biotech (Beijing,China); and the miRNA primers were designed and synthesized by Changchun Jing Mei Biological Engineering Co. Ltd. (Changchun, China).

Instruments: The Nanodrop 2000 ultra-micro spectrophotometer (Thermo, USA), Stepone quantitative PCR instrument (ABI, USA); and Bioptic Qsep100 automatic nucleic acid analyzer (BiOptic, Taiwan).

RT and q-PCR detection of miRNA expression: The miRNA extracted from the plasma was reverse transcribed into cDNA according to the instructions provided in the Takara reverse transcription kit. The corresponding RT primers were then added. The subsequent quantitative-polymerase chain reaction (q-PCR) was carried out using the SYBR Green PCR kit with the synthesized cDNA as the template. The reaction conditions were as follows: preheating at 95°C for 10 min, followed by heating at 95°C for 15 s and 60°C for 1 min with a total of 40 cycles. Using U6 as the reference, the Ct value, dissolution curve, and amplification curve of the samples were analyzed after the experiment.The following primer sets were used for qRT-PCR: miR4638-3P:TGGACACCGCTCAGCCGG; miR1273g-3P:ACCACTGCACTCCAGCCTGAG; U6:CTCGCTTCGGCAGCACA.

Statistical analyses

The SPSS 17.0 statistical software was used for data analysis. The measurement data with normal distribution are expressed as mean ± standard deviation ($X \pm SD$), and two-independent-sample *t* test was used for comparison between groups. The measurement data with non-normal distribution are expressed as median (interquartile range, IQR), and Wilcoxon rank sum test was used for comparison between groups. The χ^2 test was used to compare the enumeration data between the groups. The difference was statistically significant when $P < 0.05$.

Results

DEGs and analysis of their biological functions

A total of 19 cases (5 cases for group A, 10 cases for group B, and 4 cases for group C) were found to be qualified for the study after strict filtering and screening of the GSE40447 data. Among the three groups, the 19 blood samples were assessed. Compared with that of group B, group A had 2282 DEGs, including 1321 up-regulated DEGs and 961 down-regulated DEGs. Compared with that of group C, group A had

1195 DEGs, including 752 up-regulated DEGs and 443 down-regulated DEGs. Compared with that of group C, group B had 1718 DEGs, including 525 up-regulated DEGs and 1193 down-regulated DEGs. The DGE analysis among groups A, B, and C showed that there were 30 intersection genes (Table 1).

Note: Bold font indicates that the trends of the gene in group A were opposite to those in groups B and C. Red represents up-regulation of group A genes and down-regulation of groups B and C genes; green represents down-regulation of group A genes and up-regulation of groups B and C genes.

GO and signaling pathway analyses

The GO analysis of the 30 intersection genes from the three groups revealed that the biological functions of these genes mainly included cell-cell adhesion, response to toxic substance, and lipid catabolic process (Figure 1). The cellular components mainly included cytosol, nuclear speck, and cell-cell adhesion junction (Figure 2). The molecular functions included cadherin binding involved in cell-cell adhesion and phospholipid binding (Figure 3). The signaling pathways found in the KEGG database showed that these target genes are mainly distributed in the hippocampus-dependent long-term potentiation and long-term depression pathways, intercellular gap junction pathway, gonadotropin-releasing hormone signal transduction pathway, and circadian entrainment pathway (Figure 4).

The differentially expressed mRNA was predicted using the miRanda and TargetScan software, and 2978 miRNAs were obtained by taking the intersections. After comparing groups A, B, and C, the genes with significant differences between group A and groups B and C (*PHLDB2*, *LINC01590*, *SMIM8*, *CENPT*, *VPS53*, *ITGB8*, *TTC26*, *PGM5-AS1*, *GKAP1*, *ZNF736*, and *GPATCH2*) were selected for miRNA prediction. A total of 908 miRNAs were predicted.

To analyze the miRNA-target gene regulatory network, the targeted regulatory relationship between the miRNA and target genes was used to construct the miRNA-gene interaction network. According to the screening results based on score > 175, Energe<-35, the predicted miRNAs of the above genes included hsa-miR-4638-3p, hsa-miR-5096, hsa-miR-4763-5p, hsa-miR-1273g-3p,hsa-miR6192, hsa-miR-4726-5p, and hsa-miR-1273a. They had higher centrality toward the genes *VPS53, PHLDB2, GPATCH2, ITGB8, ZNF736, TTC26* and *CENPT*. Among them, hsa-miR-4638-3p and hsa-miR-1273g-3p exhibited the highest centrality (Table 2).

hsa-miR-4638-3p and hsa-miR-1273g-3p were analyzed for intersection of target genes and signaling pathways. There were 1947pcs of intersection genes of hsa-miR4638-3p and hsa-miR-1273g-3p for signaling pathway analysis. TGF-β signaling pathway and adhesion signaling pathway were involved in cardiotoxicity, and 45pcs of intersection genes were closely related to these two pathways. ROCK1 and MAPK1 are two key genes in the pathway (Figure 5).

Demographic and baseline cardiovascular pa[1]rameters are shown in Table 3.Taking U6 as the internal reference, for statistical convenience, the expression level of hsa-miR-4638-3p and hsa-miR-1273g-3p in the peripheral blood was calculated by the $2^{-\triangle\triangle ct}$ method. Their expression levels relative to that of U6

were converted to Log_2 ΔCt values. The expression of hsa-miR-4638-3p and hsa-miR-1273g-3p in the peripheral blood of the 20 subjects is presented in Table 4.

Discussion

The mechanism of anthracycline-induced cardiotoxicity has not been fully understood. The existing evidences reveal that it is directly related to the free radicals produced by anthracyclines [4,5]. Unlike their mechanism of anti-tumor activity, the main mechanisms of anthracycline-induced cardiotoxicity involve iron-mediated production of reactive oxygen species (ROS) and the promotion of myocardial oxidative stress. Anthracyclines chelate iron ions and trigger the generation of oxygen free radicals, especially the hydroxyl free radicals, resulting in lipid peroxidation of myocardial cell membrane, myocardial mitochondrial DNA damage, etc [6,7]. The other mechanisms include the formation of toxic drug metabolites, inhibition of nucleotide and protein synthesis, release of vasoactive amines, suppression of specific gene expression, impairment of mitochondrial membrane binding, aggregation of creatine kinase activity, induction of apoptosis, interference of intracellular calcium homeostasis, changes in respiratory chain proteins, induction of nitric oxide synthase, enhancement of mitochondrial cytochrome C release, etc [8,9]. Other studies have shown that anthracyclines can lead to myocardial cell damage, inducing cardiac mitochondrial diseases and impairment of mitochondrial DNA and the respiratory chain in chronic cardiomyopathy [10-12]. However, a solution to this problem is yet to be identified. One of the main reasons behind this is that the mechanism of pathogenesis of anthracycline-induced diseases is not fully understood. Modern medical studies have shown that it is difficult to fully explain the origin and development of a disease using the results regarding a single gene or signaling pathway. High-throughput biological detection technology, or gene chip detection technology, can obtain a large amount of gene expression information simultaneously. We can understand the biological molecules in living cells and their interactions by analyzing such gene expression information through bioinformatic methods. This way, the key factors involved in the pathogenesis of diseases can be identified, which can serve as references for target design in clinical treatment [13].

Recent studies have shown that miRNA is involved in the processes of regulating the growth and development, mechanical remodeling, and electrical remodeling of the heart and is closely related to heart diseases [14]. The overexpression of miRNA-1 and miRNA-133 can inhibit cardiomyocyte hypertrophy [15]. Up-regulated miRNA-21 due to myocardial emergency can lead to fibroblast proliferation and myocardial interstitial fibrosis via the activation of extracellular ERK/MAPK signaling pathways by targeted inhibition of the expression of RAS/MEK/ERK inhibitor SPRY1 [16]. miRNA-29, miRNA-133, and miRNA-30 have also been proved to be involved in cardiac fibrosis. Terentyev et al. [17] showed that miRNA-1 can also act on the regulatory subunit b56α of protein phosphatase PP2A, releasing PP2A from the L2-type calcium channel in cardiomyocyte membrane and causing the phosphorylation of Ca^{2+}/calmodulin-dependent protein kinase II (CaMK II), which leads to the activation of RyR2 in the sarcoplasmic reticulum. This enhances the release of calcium ions and promotes cardiac arrhythmogenesis. Wijnen et al. [18] evaluated the role of miRNA in myocardial fibrosis using a specific

miRNA transgenic mouse model and methods such as the loss-of-function and gain-of-function. The results revealed that the miRNA can directly target the transforming growth factor beta receptor (TGFBR) to promote the formation of types I and II receptor complexes and activate the TGF-β signaling pathway to induce the increased secretion of collagen, while AMO can eliminate such effect.

In the present study, we used the raw data of GSE40447 gene chip in the GEO database and adopted software packages to analyze differentially expressed miRNAs. The DGE analysis between group A and groups B and C showed that there were 30 intersection genes. With further analysis of the biological functions and signaling pathways, it was found that the main functions of the differentially expressed miRNA-mRNA included cell-cell adhesion, response to toxic substance, and lipid catabolic process. Their cellular components mainly included cytosol, nuclear speck, and cell-cell adhesion junction. The genes *VPS53, ITGB8, ZNF736,* and *TTC26* play important roles in cholesterol transport in cardiac cells, mediating the interaction between cell-cell and cell-extracellular matrix, regulate transcription, and transport proteins[19-21]. Among them *VPS53* and *PHLDB2, GPATCH2, ITGB8, ZNF736, TTC26* exhibited opposite expressions in groups A, B, and C. This suggests that *VPS53* and *PHLDB2, GPATCH2, ITGB8, ZNF736, TTC26* might have opposite effects on some processes of the disease. The molecular functions included cadherin binding involved in cell-cell adhesion and phospholipid binding. The signaling pathways found in the KEGG database showed that these target genes were mainly distributed in the hippocampus-dependent long-term potentiation and long-term depression pathways, intercellular gap junction pathway, gonadotropin-releasing hormone signal transduction pathway, and circadian entrainment pathway. The biological functions of miRNA were mainly realized through the regulation and control of their target genes. The analysis of the functions of these differentially expressed miRNAs revealed that hsa-miR-4638-3p, hsa-miR-5096, hsa-miR-4763-5p, hsa-miR-1273g-3p, hsa-miR6192, hsa-miR-4726-5p, and hsa-miR-1273a have higher centrality. This indicates that these miRNA targets are extensive, including oncogenes, tumor suppressor genes, signal transduction genes, and cell cycle regulation genes. Therefore, target gene prediction can provide a theoretical basis for further target gene verification experiments and avoid blind obedience. Further analysis of the miRNA-target gene regulatory network also showed that the miRNAs such as hsa-miR-4638-3p and hsa-miR-1273g-3p had the highest centrality to the surrounding target genes, suggesting that they are the core regulatory miRNAs. The PCR results were consistent with the predicted results. The results of clinical sample validation showed that there was a significant difference between hsa-miR4638-3P and hsa-1273 before and after anthracycline chemotherapy. According to GO annotation and signal pathway analysis, ROCK1 and ERK are two key genes in the pathway, which may regulate the cardiac toxicity of anthracycline drugs through TGF-β signaling pathway and adhesion signaling pathway. Rho kinase (ROCK) is one of the downstream effectors of small G protein Rho. The Rho-ROCK pathway plays an important role in mediating various cellular functions, including contraction, actin cytoskeleton, cell adhesion and movement, proliferation, cytokinesis, and gene expression, all of which are involved in the pathogenesis of cardiovascular disease[22,23]. RHO/ROCK specific inhibitors show promise in the prevention of heart disease. ROCK1 is activated after cardiomyocytes are treated with doxorubicin in vitro, and RHO/ROCK inhibitors can prevent doxorubicin cardiotoxicity[24]. ROCK1 mediates autophagy dysregulation and apoptosis in

adriamycin cardiotoxicity, and promotes cardiac remodeling and reverse dysfunction [25]. ERK activation provides a possible mechanism to prevent doxorubicin-induced cardiomyocyte injury[26-28]. These observations suggest that some medicine can prevent doxorubicin cardiotoxicity by inhibiting oxidative stress, restoring cardiac mitochondrial function or stimulating ERK activation.

The present study had some limitations. Based on the results of bioinformatic analysis, we can predict numerous target genes. However, there are also some false positives; therefore, its accuracy needs further validation by molecular biology experiment, in order to identify the real target genes of each miRNA and to verify the exact role played by miRNA in the development and incidence of anthracycline-induced cardiac toxicity. In the verification experiment,The number of cases collected in this experiment is small, and the experimental results have certain limitations. The reliability of the data needs to be further expanded to confirm the sample size.

Abbreviations

EF:Ejection fraction;FC:Fold change;FDR:False discovery rate;GO:Gene Ontology

KEGG:Kyoto Encyclopedia of Genes and Genomes;miRNA：MicroRNA; cDNA:complementary DNA; q-PCR:quantitative-polymerase chain reaction; IQR:interquartile range; *PHLDB2*:pleckstrin homology like domain family B member 2; *LINC01590*:long intergenic non-protein coding RNA 1590; *SMIM8*:small integral membrane protein 8; *CENPT*:centromere protein T;*VPS53*:VPS53 subunit of GARP complex; *ITGB8*:integrin subunit beta 8; *TTC26*:tetratricopeptide repeat domain 26; *PGM5-AS1*:PGM5 antisense RNA 1; *GKAP1*:G kinase anchoring protein 1; *ZNF736*:zinc finger protein 736; *GPATCH2*:G-patch domain containing 2; *ROCK1*:Rho associated coiled-coil containing protein kinase 1; ERK: mitogen-activated protein kinase 1;CaMK II:Ca^{2+}/calmodulin-dependent protein kinase II ; *SPRY1*: sprouty RTK signaling antagonist 1; RyR2:ryanodine receptor 2;TGFBR:transforming growth factor beta.

Declarations

Acknowledgments

This manuscript has been edited and proofread by CACTUS Editage Bioscience Limited.

Authors' contributions

WYD and HDN conceived and designed the study. CSR, ZT, TQ and CSX performed the experiments and statistical analysis. WYD wrote the paper. CSX and HDN reviewed and edited the manuscript. All authors read and approved the manuscript.

Funding

This work was supported by the Natural Science Foundation of Liaoning Province of China NO.20170540384. The funders had no role in study design, data collection and analysis, decision to

publish or preparation of the manuscript.

Availability of data and materials

The data used to support the findings of this study are available from the corresponding author upon request.

Ethics approval and consent to participate

Approved by Medical Ethics Committee of TThe Third Affiliated Hospital, Jinzhou Medical Universit. Approval Number: 2017-005

Consent for publication

Not applicable.

Competing interests

The authors declare that they have no competing interests, and all authors should confirm its accuracy.

References

[1]Vejpongsa P, Yeh ET. Prevention of anthracycline-induced cardiotoxicity: challenges and opportunities.J Am Coll Cardiol. 2014,64(9):938-945. https://doi.org/10.1016/j.jacc.2014.06.1167

[2]Caron J, Nohria A.Cardiac Toxicity from Breast Cancer Treatment: Can We Avoid This?.Curr Oncol Rep. 2018,20(8):61. https://doi.org/10.1007/s11912-018-0710-1.

[3]Ye J,Fang L, Zheng H,et al. WEGO a web tool for plotting GO annotations.Nucleic Acids Res. 2006,34(Web Server issue):W293-297. https://doi.org/10.1093/nar/gkl031

[4] D. Cappetta, A. De Angelis, L. Sapio, et al., 2017.Oxidative stress and cellular response to doxorubicin: a common factor in the complex milieu of anthracycline cardiotoxicity. Oxid. Med. Cell Longev. 2017, 1521020. https://doi.org/10.1155/2017/1521020.

[5] R.W. Loar, C.V. Noel, H. Tunuguntla, et al., State of the art review: chemotherapy-induced cardiotoxicity in children, Congenit. Heart Dis. 13 (2017) 5–15. https://doi.org/10.1111/chd.12564.

[6] T. Simunek, M. Stérba, O. Popelov, et al., Anthracycline-induced cardiotoxicity: overview of studies examining the roles of oxidative stress and free cellular iron, Pharmacol. Rep.61 (2009) 154–171. https://doi.org/10.1016/S1734-1140(09)70018-0.

[7] X. Xu, H.L. Persson, D.R. Richardson, Molecular pharmacology of the interaction of anthracyclines with iron, Mol. Pharmacol. 68 (2005) 261–271. https://doi.org/10.1124/mol.105.013383.

[8] E. Barry, J.A. Alvarez, R.E. Scully, et al., Anthracycline-induced cardiotoxicity: course, pathophysiology, prevention and management, Expert Opin. Pharmacother. 8 (2007) 1039–1058. https://doi.org/10.1517/14656566.8.8.1039.

[9] S.L. Leong, N. Chaiyakunapruk, S.W. Lee, Candidate gene association studies of anthracycline-induced cardiotoxicity: a systematic review and meta-analysis, Sci Rep. 7 (2017) 39. https://doi.org/10.1038/s41598-017-00075-1.

[10] K.B. Wallace, Doxorubicin-induced cardiac mitochondrionopathy, Pharmacol. Toxicol. 93 (2003) 105–115. https://doi.org/10.1034/j.1600-0773.2003.930301.x.

[11] D. Lebrecht, U.A. Walker, Role of mtDNA lesions in anthracycline cardiotoxicity, Cardiovasc. Toxicol. 7 (2007) 108–113. https://doi.org/10.1007/s12012-007-0009-1.

[12] D. Lebrecht, A. Kokkori, U.P. Ketelsen, et al., Tissue-specific mtDNA lesions and radical-associated mitochondrial dysfunction in human hearts exposed to doxorubicin, J.Pathol. 207 (2005) 436–444. https://doi.org/10.1002/path.1863.

[13] P.A. Jones, J.P. Issa, S. Baylin, Targeting the cancer epigenome for therapy, Nat. Rev. Genet. 17 (2016) 630–641. https://doi.org/10.1038/nrg.2016.93.

[14] T.E. Callis, Wang DZ, Taking microRNAs to heart, Trends Mol. Med. 14 (2008) 254–260. https://doi.org/10.1016/j.molmed.2008.03.006.

[15] G.B. Fogel, Z.S. Kai, S. Zargar, et al., MicroRNA dynamics during human embryonic stem cell differentiation to pancreatic endoderm, Gene. 574 (2015) 359–370. https://doi.org/10.1016/j.gene.2015.08.027.

[16] J.N. Zhu, Y.H. Fu, Z.Q. Hu, et al., 2017. Activation of miR-34a-5p/Sirt1/p66shc pathway contributes to doxorubicin-induced cardiotoxicity. Sci. Rep. 7, 11879. https://doi.org/10.1038/s41598-017-12192-y.

[17] D. Terentyev, A.E. Belevych, R. Terentyeva, et al., miR21 overexpression enhances Ca^{2+} release and promotes cardiac arrhythmogenesis by targeting PP2A regulatory subunitB56 and causing caMK□-dependent hyperphosphorylation of RyR2, Circ. Res. 104 (2009) 514–521. https://doi.org/10.1161/CIRCRESAHA.108.181651.

[18] W.J. Wijnen, Y.M. Pinto, E.E. Creemers., 2013. The therapeutic potential of miRNAs in cardiac fibrosis: where do we stand? J Cardiovasc. Transl. Res. 6 (6) 899–908. https://doi.org/10.1007/s12265-013-9483-y.

[19]Ishikawa H, Ide T, Yagi T,et al.TTC26/DYF13 is an intraflagellar transport protein required for transport of motility-related proteins into flagella. Elife. 2014 ,3:e02897. doi: 10.7554/eLife.02897.

[20]Pérez-Victoria FJ, Mardones GA, Bonifacino JS.Requirement of the human GARP complex for mannose 6-phosphate-receptor-dependent sorting of cathepsin D to lysosomes. Mol Biol Cell. 2008 ,19(6):2350-62. doi: 10.1091/mbc.E07-11-1189.

[21]Wei J, Zhang YY, Luo J.et al.The GARP Complex Is Involved in Intracellular Cholesterol Transport via Targeting NPC2 to Lysosomes.Cell Rep. 2017,27;19(13):2823-2835.

doi: 10.1016/j.celrep.2017.06.012

[22]Shimokawa H, Rashid M. Development of Rho kinase inhibitors for cardiovascular medicine.Trends Pharmacol Sci. 2007,28(6):296-302.doi: 10.1016/j.tips.2007.04.006

[23]Surma M, Wei L, Shi J.Rho kinase as a therapeutic target in cardiovascular disease.Future Cardiol. 2011,7(5):657-71.doi: 10.2217/fca.11.51

[24]Sysa-Shah P, Xu Y, Guo X, Pin S, Bedja D, Bartock R, Tsao A, Hsieh A, Wolin MS, Moens A, Raman V, Orita H, Gabrielson KL.Geranylgeranylacetone blocks doxorubicin-induced cardiac toxicity and reduces cancer cell growth and invasion through RHO pathway inhibition. Mol Cancer Ther. 2014,13(7):1717-728. doi: 10.1158/1535-7163.

[25]Shi J, Surma M, Wei L. Disruption of ROCK1 gene restores autophagic flux and mitigates doxorubicin-induced cardiotoxicity. Oncotarget. 2018,9(16):12995-13008. doi:10.18632/oncotarget.24457.

[26]Huang CY, Chen JY, Kuo CH, Pai PY, Ho TJ, Chen TS, Tsai FJ, Padma VV, Kuo WW, Huang CY.Mitochondrial ROS-induced ERK1/2 activation and HSF2-mediated AT1 R upregulation are required for doxorubicin-induced cardiotoxicity. J Cell Physiol. 2018,233(1):463-475. doi:10.1002/jcp.25905.

[27]Yang L, Luo C, Chen C, Wang X, Shi W, Liu J.All-trans retinoic acid protects against doxorubicin-induced cardiotoxicity by activating the ERK2 signalling pathway. Br J Pharmacol. 2016,173(2):357-71.doi:10.1111/bph.13377.

[28]Eldridge S, Guo L, Mussio J, Furniss M, Hamre J 3rd, Davis M.Examining the protective role of ErbB2 modulation in human-induced pluripotent stem cell-derived cardiomyocytes.Toxicol Sci. 2014,141(2):547-59. doi:10.1093/toxsci/kfu150.

Tables

Table 1 List of intersection genes with differential gene expression in groups A, B, and C

Number	Gene symbol	Avs.B FC	Avs.C FC	Bvs.C FC	Style
1	MAPK1	1.33	1.39	-1.46	
2	NPHP3	1.33	1.34	1.49	
3	ARL17A	-1.62	-1.67	1.41	
	ARL17B	-1.62	-1.67	1.41	
	LOC100294341	-1.62	-1.67	1.41	
	LOC100996709	-1.62	-1.67	1.41	
4	MBP	1.51	1.55	1.43	
5	RABGAP1L	-1.23	-1.28	-1.55	
6	PHLDB2	-1.51	1.24	1.69	
7	PECAM1	1.35	1.26	1.42	
8	PVT1	-1.35	-1.27	-1.23	
9	ITGB8	1.41	-1.37	-1.41	
10	LIPJ	1.30	1.26	1.29	
11	ATXN2L	1.62	1.63	-1.44	
12	TCEB3	1.48	1.45	-1.42	
13	CTIF	1.57	1.42	1.22	
14	OSBPL1A	1.47	1.29	-1.37	
15	LINC01590	-1.65	1.45	1.58	
	SMIM8	-1.65	1.45	1.58	
16	PLCB1	1.22	1.29	1.56	
17	CENPT	1.37	-1.37	-1.35	

18	ENGASE	1.27	1.68	1.33
19	FAM27B	1.36	2.22	1.64
	FAM27C	1.36	2.22	1.64
	LOC102725186	1.36	2.22	1.64
	LOC105379444	1.36	2.22	1.64
20	SPTBN1	-1.56	-1.33	1.54
21	**VPS53**	**1.29**	**-1.58**	**-1.31**
22	RNF34	1.32	1.54	-1.36
23	**PGM5-AS1**	**-1.31**	**2.00**	**1.34**
24	FGFR1OP2	-1.47	-2.28	-2.27
25	**GKAP1**	**-1.67**	**1.42**	**1.29**
26	**ZNF736**	**-1.79**	**1.27**	**1.36**
27	**TTC26**	**-1.79**	**1.42**	**1.73**
28	TSHZ2	-1.79	-2.20	-1.66
29	DUSP8	1.39	1.47	1.30
30	**GPATCH2**	**-1.6**	**1.24**	**1.29**

Table 2 miRNA prediction of genes with significant differences between group A and groups B and C

Gene Symbol	microRNA	Score	Energe
VPS53	hsa-miR-4638-3p	193	-45.14
	hsa-miR-5096	191	-38.75
	hsa-miR-7851-3p	184	-32.95
	hsa-miR-4763-5p	183	-38.27
	hsa-miR-2110	178	-34.93
	hsa-miR-1200	176	-29.67
	hsa-miR-619-5p	**175**	**-33.81**
ITGB8	hsa-miR-4729	179	-22.78
	hsa-miR-1208	177	-26.73
	hsa-miR-1273e	176	-29.11
	hsa-miR-136-3p	175	-21.8
PHLDB2	hsa-miR-1273g-3p	195	-43.01
	hsa-miR6192	175	-36.3
GPATCH2	hsa-miR-1273g-3p	195	-41.57
	hsa-miR-1273a	183	-31.32
ZNF736	hsa-miR-3189-3p	175	-31.94
TTC26	hsa-miR-1273a	187	-36.01
CENPT	hsa-miR-4726-5p	175	-35.1

Table 3 Classification and Baseline Values of Patients

Group	A	C	
N	20	20	
chemotherapy	No	Yes	
Low Ejection Fractions	No	Yes	
Age(median, range)	54(35-75)	54(35-75)	NS
Ejection Fractions,EF(median)	48	68	P < 0.001
Hypertension	No	No	NS
Diabetic	No	No	NS

Note:Group A: women diagnosed with breast cancer and anthracycline induced cardiotoxicity; group C: women diagnosed with breast cancer but with normal ejection fraction before chemotherapy.

Table 4 Expression level of hsa-miR-4638-3p and hsa-miR-1273g-3p in the peripheral blood of each group (Log_2 $^{\Delta}$Ct value)

		Mean value (X ± SD)	
Group	N	hsa-miR-4638-3p	hsa-miR-1273g-3p
A	20	1.2993±0.7920	0.996±0.1975
C	20	2.6424±1.4019 *	0.4763±0.1817*
		P=0.008	*P*=0.000

Note: independent-sample t test was adopted: $^{*}P < 0.05$. Group A: women diagnosed with breast cancer and anthracycline-induced cardiotoxicity; group C: women diagnosed with breast cancer but with normal ejection fraction before chemotherapy.

Figures

Figure 1

Biological functions of the differentially expressed intersection genes

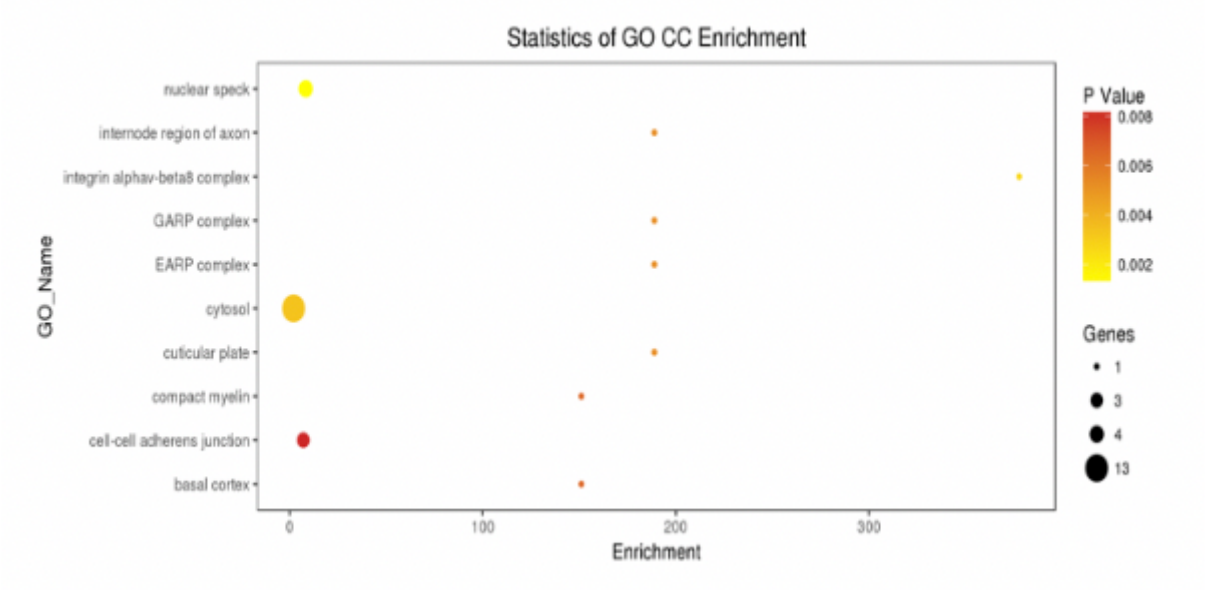

Figure 2

Cellular components of the differentially expressed intersection genes

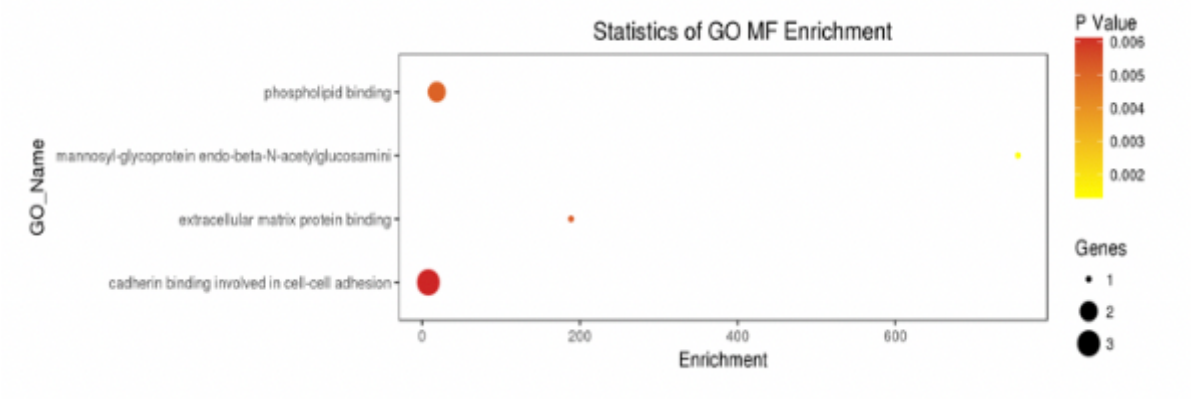

Figure 3

Molecular functions of the differentially expressed intersection genes

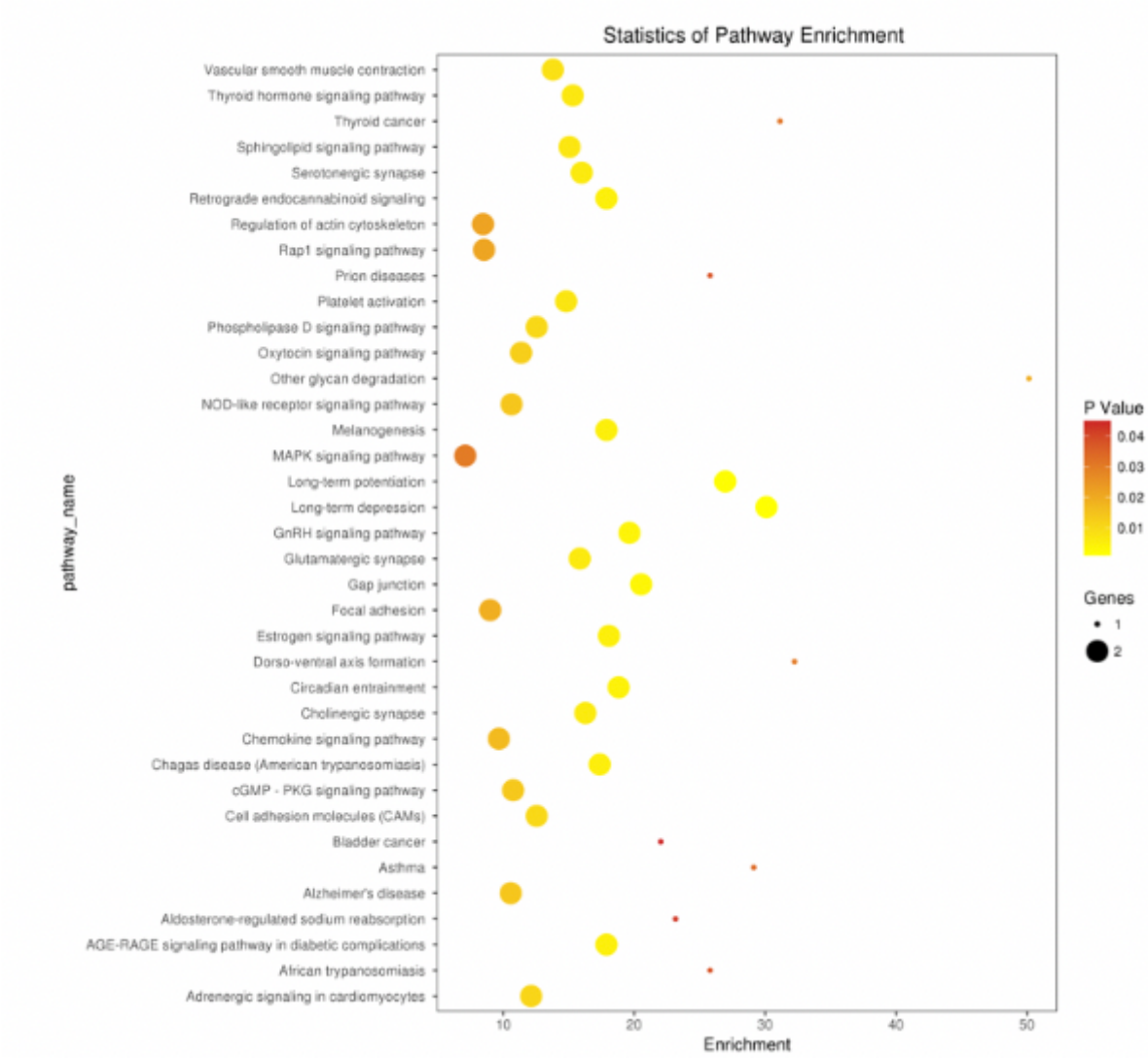

Figure 4

Signaling pathways of the differentially expressed intersection genes miRNA prediction of intersection genes

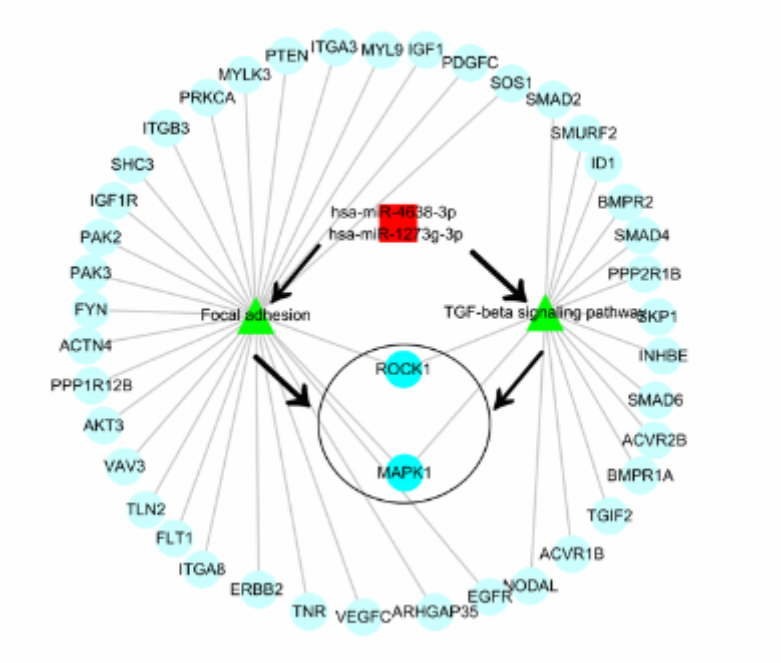

Figure 5

hsa-miR-4638-3p and hsa-miR-1273g-3p Target Gene Network Map PCR verification